Differential scattering cross section of the non-Abelian Aharonov-Bohm effect in multiband systems

Róbert Németh * and József Cserti
Department of Physics of Complex Systems, ELTE Eötvös Loránd University, H-1117 Budapest, Pázmány Péter sétány 1/A, Hungary

(Received 1 July 2023; accepted 14 September 2023; published 2 October 2023)

We develop a unified treatment of the non-Abelian Aharonov-Bohm (AB) effect in isotropic multiband systems, namely, the scattering of particles on a gauge field corresponding to a noncommutative Lie group. We present a complex contour integral representation of the scattering states for such systems, and using their asymptotic form, we calculate the differential scattering cross section. The angular dependence of the cross section turns out to be the same as that obtained originally by Aharonov and Bohm in their seminal paper [Phys. Rev. **115**, 485 (1959)], but this time, it depends on the polarization of the incoming plane wave. As an application of our theory, we perform the contour integrals for the wave functions explicitly and calculate the corresponding cross section for three nontrivial isotropic multiband systems relevant to condensed matter and particle physics. To have a deeper insight into the nature of the scattering, we plot the probability and current distributions for different incoming waves. This paper is a generalization of our recent results on the Abelian AB effect providing an extension of exactly solvable AB scattering problems.

DOI: 10.1103/PhysRevB.108.155402

I. INTRODUCTION

Aharonov and Bohm in their seminal paper [1] calculated how the incident plane wave of a spinless free particle is scattered by an infinitely thin magnetic solenoid and the differential scattering cross section. The experimental verification of this quantum effect was reported by Chambers [2], while the mathematical details of the theory were further explored by Berry [3] and Berry *et al.* [4]. The scattering problem was also generalized in the framework of relativistic quantum mechanics by Alford and Wilczek [5], by de Sousa Gerbert [6], and also by Hagen [7] and Hagen and Ramaswamy [8]. The non-Abelian version of the Aharonov-Bohm (AB) effect in which the magnetic field responsible for the scattering is replaced by an SU(2) gauge field has been studied by Wu and Yang [9], and by Horváthy [10]. They discussed the analogies of both the original AB scattering problem and the interference pattern forming in two-slit geometries such as in the experiment of Chambers [2]. Lately, the theory was also extended to the case of time-dependent gauge fields [11,12]. However, only a limited number of specific systems have been discussed, and a general formalism has never been developed.

Recently, the realization of non-Abelian gauge potentials in optical lattices was studied extensively [13–20], with special interest toward the non-Abelian AB effect [21–26]. Additionally, Yang *et al.* [27] reported the successful observation of the SU(2) AB phase shift using optical interferometry. Therefore, the role of gauge fields is becoming more and more significant in the current research of condensed matter physics.

In our recent work [28], based on a contour integral formalism, we developed a general theory of the Abelian AB effect for multiband systems possessing isotropic dispersion relations to obtain the scattering states and the differential cross section. As a striking result, it turned out that the cross section has the same functional form for all isotropic systems and is identical to that derived by Aharonov and Bohm [1]. In this paper, as an extension, we develop a general theory for the case of non-Abelian scattering potentials. We find that the cross section again has the same dependence on the polar angle φ as in the Abelian case and is given by

$$\sigma_{\mathrm{AB,gen}}(\varphi) = \frac{\Sigma}{2\pi k \cos^2(\varphi/2)}, \tag{1}$$

where Σ is a numerical factor depending on the non-Abelian nature of the flux and the incoming wave function. The detailed derivation of this result is presented in the following sections. To see how our approach can be used in practice, we shall consider three simple examples relevant to both solid-state and particle physics. However, more complicated multiband systems can be treated in a similar fashion.

The paper is structured as follows. In Sec. II, we present the general results of our theory. Specifically, in Sec. II A, we introduce the basic notions of gauge theory needed to define the scattering problem; in Sec. II B, we describe the set of systems our approach is applicable to; in Sec. II C, we give a general formula for the scattering states using an integral representation; and in Sec. II D, we derive the differential scattering cross section and discuss similarities and differences compared with the Abelian case. In Sec. III, our method is applied to one- and two-band systems, and explicit expressions of both the scattering states and the differential cross section are presented. We consider the case of an SU(2) doublet in Sec. III A, an SU(3) triplet in Sec. III B, and a U(2) doublet in Sec. III C.

II. GENERAL THEORY

In this section, we outline our approach to obtain the scattering states and the cross section for the non-Abelian AB effect. First, we define the most general Hamiltonian

*robert.nemeth@ttk.elte.hu

describing isotropic multiband systems. Then we propose our contour integral representation of the scattering states which is a generalization of that presented in Ref. [28]. Furthermore, we calculate the differential scattering cross section.

A. Gauge potential

In the conventional AB effect, the physical space is taken to be the two-dimensional plane with the origin removed; we denote this by $\mathbb{R}^2_\circ$. The scattering potential is introduced in the form of the magnetic vector potential which is a (co)vector field on the physical space [1,28]. Each component of this field is real, so the target space is the set $\mathbb{R}$ which can be identified with the one-dimensional Lie algebra $\mathfrak{u}(1)$ corresponding to the Lie group $\mathrm{U}(1)$ of complex numbers with absolute value one. In this way, one can think of the vector potential as a $\mathrm{U}(1)$ gauge potential.

This description allows us to create the concept of *gauge potentials* corresponding to a more general non-Abelian Lie group G. For our investigation, we restrict ourselves to groups that are locally isomorphic to a subgroup of $\mathrm{U}(N)$ around the identity element. In this case, each component of the gauge potential is an element of the Lie algebra $\mathfrak{g} \subseteq \mathfrak{u}(N)$, that is, a self-adjoint $N \times N$ complex matrix. Along these lines, the generalization of the AB vector potential to the G case is straightforward, in Cartesian components given by

$$\hat{A}_x(x,y) = -\frac{\hat{\Phi} y}{2\pi(x^2+y^2)}, \tag{2a}$$

$$\hat{A}_y(x,y) = \frac{\hat{\Phi} x}{2\pi(x^2+y^2)}. \tag{2b}$$

Here, the non-Abelian version of the flux $\hat{\Phi}$ is an element of $\mathfrak{g}$. Self-adjointness implies that $\hat{\Phi}$ is diagonal on a suitable orthonormal basis, and its eigenvalues Φ_n are real for all $n \in \{1,\ldots,N\}$.

The *gauge field* is an antisymmetric rank-2 tensor field that serves as the generalization of the magnetic field. Thus, in two dimensions, it has a single independent component given by

$$\hat{F}_{xy} = \partial_x \hat{A}_y - \partial_y \hat{A}_x + [\hat{A}_x, \hat{A}_y] = 0. \tag{3}$$

Like before, this field vanishes on $\mathbb{R}^2_\circ$. This simple model of an infinitesimally thin flux tube could be extended to a more realistic, experimentally feasible one where the gauge field is nonzero in a finite region around the origin. However, we believe that our model captures the most relevant features of the scattering provided that the characteristic wavelength of the particles is much larger than the tube.

For the Abelian case, the line integral of the gauge potential equals the flux for an arbitrary closed curve C once encircling the origin anticlockwise. For the non-Abelian case, however, we should instead use the path-ordered exponential of the gauge potential called the *Wilson loop operator*:

$$\hat{W} = \mathrm{P}\exp\left[\frac{ie}{\hbar}\oint_C \hat{\mathbf{A}}\right] = \exp(2\pi i\hat{\alpha}), \tag{4}$$

where we introduced the dimensionless flux $\hat{\alpha} = \hat{\Phi}/\Phi_0$ with $\Phi_0 = h/e$. In summary, the infinitesimal flux tube has similar properties in the Abelian and non-Abelian cases, but for the latter, the matrix nature of the flux must be kept in mind.

B. Hamiltonian operator

The most general Hilbert space of the systems we study in this paper takes the form $\mathcal{H} = L^2(\mathbb{R}^2) \otimes \mathbb{C}^N \otimes \mathbb{C}^D$, consisting of the two-dimensional spatial, N-dimensional gauge, and a D-dimensional internal degrees of freedom. The gauge degree of freedom is also referred to as *polarization*. Furthermore, we limit ourselves to studying Hamiltonians satisfying the three requirements mentioned in our previous paper [28]: *polynomicity*, *isotropy*, and *regularity*. Thus, the Hamiltonian operator in the absence of the gauge field takes the form:

$$\hat{H} = \sum_{i=0}^{I}\sum_{j=0}^{J} \hat{p}_x^i \hat{p}_y^j \otimes \hat{I}_N \otimes \hat{T}_{ij}, \tag{5}$$

where $\hat{T}_{ij}$ is a $D \times D$ self-adjoint matrix for each i, j, and $\hat{I}_N$ is the $N \times N$ identity matrix. In the presence of the gauge field, we need to introduce the kinetic momentum operators acting on the direct product Hilbert space $L^2(\mathbb{R}^2) \otimes \mathbb{C}^N$:

$$\hat{\Pi}_x = \hat{p}_x \otimes \hat{I}_N + \hat{A}_x(\hat{x},\hat{y}), \tag{6a}$$

$$\hat{\Pi}_y = \hat{p}_y \otimes \hat{I}_N + \hat{A}_y(\hat{x},\hat{y}). \tag{6b}$$

Here, the components of the gauge potential from Eq. (2) are used. Then the total Hamiltonian in the presence of the gauge field reads

$$\hat{H} = \sum_{i=0}^{I}\sum_{j=0}^{J} \hat{\Pi}_x^i \hat{\Pi}_y^j \otimes \hat{T}_{ij}. \tag{7}$$

C. Scattering states

As in our previous work [28], here, we construct the contour integral representation of the scattering states for the non-Abelian AB effect. To this end, we need the eigenvectors of the Hamiltonian in Eq. (7) in the absence of the gauge field. These are plane waves with wave number $\mathbf{k} = k(\cos\vartheta, \sin\vartheta)$, definite polarization $\mathbf{w}_n \in \mathbb{C}^N$, and internal degree of freedom $\mathbf{u}_s(\mathbf{k}) \in \mathbb{C}^D$ given by

$$\mathbf{\Psi}_{s,n,\mathbf{k}}(r,\varphi) = \exp[ikr\cos(\varphi-\vartheta)]\mathbf{w}_n\mathbf{u}_s(\mathbf{k}). \tag{8}$$

The corresponding eigenvalues $E_s(k)$ consists of N-fold degenerate bands owing to the different polarizations. Without the loss of generality, we can choose the vectors $\mathbf{w}_n$ such that they are eigenvectors of $\hat{\alpha}$ with eigenvalues $\alpha_n = \Phi_n/\Phi_0$:

$$\hat{\alpha}\mathbf{w}_n = \alpha_n \mathbf{w}_n. \tag{9}$$

This implies that they are eigenvalues of the Wilson loop operator $\hat{W}$ as well:

$$\hat{W}\mathbf{w}_n = \exp(2\pi i\alpha_n)\mathbf{w}_n. \tag{10}$$

Now, the scattering states satisfying the necessary requirements (i)–(iii) detailed in our paper [28] are given by

$$\mathbf{\Psi}^{(+)}_{s,n,\mathbf{k}}(r,\varphi) = \sum_{m=-\infty}^{\infty} \frac{\epsilon(m+\alpha_n)}{2\pi} \int_{\Gamma(m+\alpha_n,\varphi)} d\xi\ \mathbf{\Psi}_{s,n,\mathbf{K}}(r,\varphi) \times \exp\left[im(\xi-\vartheta) - i\alpha_n(\varphi-\xi)\right], \tag{11}$$

where $\epsilon(x)$ is the sign function defined as $\epsilon(x) = 1$, if $x \geqslant 0$, and $\epsilon(x) = -1$, if $x < 0$. Furthermore, $\mathbf{K} = k[\cos\xi, \sin\xi]$, with ξ being a complex integration variable. The integration

contours $\Gamma(m+\alpha_n,\varphi)$ are curves on the complex plane depending on the sign of $m+\alpha_n$ and the value of the real-space polar angle φ:

$$\Gamma(m+\alpha_n,\varphi)=\begin{cases}\Gamma_+(\varphi), & \text{if } m+\alpha_n \geqslant 0,\\ \Gamma_-(\varphi), & \text{if } m+\alpha_n < 0.\end{cases} \tag{12}$$

The curves $\Gamma_+(\varphi)$ and $\Gamma_-(\varphi)$ further depend on the sign of the radial component $v_{s,k}$ of the group velocity:

$$\mathbf{v}_s=\frac{1}{\hbar}\frac{\partial E_s}{\partial \mathbf{k}}. \tag{13}$$

If $v_{s,k}>0$, the curve $\Gamma_+(\varphi)$ is $\cup$-shaped, running from $\xi=-5\pi/2+\varphi+i\infty$ to $\xi=-\pi/2+\varphi+i\infty$, with $\mathrm{Re}(\xi)>0$, and the curve $\Gamma_-(\varphi)$ is $\cap$-shaped, running from $\xi=-3\pi/2+\varphi-i\infty$ to $\xi=\pi/2+\varphi-i\infty$, with $\mathrm{Re}(\xi)<0$. However, if $v_{s,k}<0$, the curve $\Gamma_+(\varphi)$ must be shifted by 2π along the real axis compared with the previous definition. Furthermore, if $v_{s,k}=0$, the scattering state has no physical meaning, as the corresponding plane waves have constant zero current density, indicating that they do not propagate.

By a straightforward generalization of the proofs given in our previous paper [28], one can show that the wave functions given by Eq. (11) are indeed proper scattering states satisfying the necessary requirements (i)–(iii) detailed there. Note that using the eigenvector basis given by Eq. (9), the non-Abelian scattering problem is decomposed into N different Abelian counterparts. Then an arbitrary incoming wave can be given as a linear combination of the wave functions in Eq. (8):

$$\mathbf{\Psi}_{\mathrm{gen}}=\sum_{n=1}^{N} c_n \mathbf{\Psi}_{s,n,\mathbf{k}}. \tag{14}$$

Hence, the same linear combination of the scattering states of Eq. (11) can be used:

$$\mathbf{\Psi}^{(+)}_{\mathrm{gen}}=\sum_{n=1}^{N} c_n \mathbf{\Psi}^{(+)}_{s,n,\mathbf{k}}. \tag{15}$$

D. Differential scattering cross section

As a usual procedure [28], using the asymptotic form of the scattering states in Eq. (11), we now calculate the differential cross section. Here, we assume that the incident particles are coming from the direction of the positive x axis. Then for given flux parameters α_n, we find that the differential cross section is

$$\sigma_{\mathrm{AB},n}(\varphi)\equiv\frac{d\sigma}{d\varphi}(s,n,k;\varphi)=\frac{\sin^2(\alpha_n\pi)}{2\pi k\cos^2(\varphi/2)}. \tag{16}$$

For an arbitrary incoming wave, the different terms in Eq. (15) are pairwise orthogonal due to the corresponding polarization vectors $\mathbf{w}_n$. Therefore, the cross section becomes a weighted sum of the terms in Eq. (16) as

$$\sigma_{\mathrm{AB,gen}}(\varphi)\equiv\frac{d\sigma}{d\varphi}(s,k;\varphi)=\frac{\Sigma}{2\pi k\cos^2(\varphi/2)}, \tag{17}$$

where we introduced the dimensionless *cross section factor* Σ given by

$$\Sigma=\sum_{n=1}^{N}|c_n|^2\,\sin^2(\alpha_n\pi). \tag{18}$$

As an important corollary, these results again show that the differential cross section is independent of the band index s and the specific form of the dispersion relation E_s provided that it is isotropic. Note that, for forward scattering, i.e., for $\varphi=\pi$, Eq. (17) is not valid due to the limitations of the saddle point approximation. This issue is present in the original AB problem and was also addressed in earlier papers [4,28]. We should also emphasize that, when the angular distribution and the polarization are measured simultaneously, the cross section will be different from that given in Eq. (17) but can easily be calculated by properly taking into account the current contributions. However, the details of this issue are not considered in this paper.

III. APPLICATIONS

In this section, we present three examples that provide more insight into the nature of the non-Abelian AB scattering problem. These examples are relevant in both condensed matter and particle physics.

A. SU(2) doublet

The first example is the SU(2) doublet. Such a system can appear in the nonrelativistic model of nucleons [29] where protons and neutrons are regarded as different isospin eigenstates of the same particle, analogously to a spin-$\frac{1}{2}$ degree of freedom [30–32]. The non-Abelian AB effect in this system has been studied before by Wu and Yang [9] and Horváthy [10]. Note that such a system is also relevant in condensed matter physics, as recently, similar systems were synthesized by trapping ultracold atoms in optical square lattices [18,25]. The low-energy dynamics of the atomic motion mimic that of two-dimensional nonrelativistic fermions. In that case, the internal degree of freedom corresponding to the isospin emerges as doubly split energy eigenstates of the cold atoms, and the gauge field is generated, for instance, by laser-assisted tunneling [24,26].

Using our methods developed in Sec. II, we now reproduce the results obtained by Horváthy [10]. The Hilbert space corresponding to the SU(2) doublet is $\mathcal{H}=L^2(\mathbb{R}^2,\mathbb{C})\otimes\mathbb{C}^2$, that is, there is no internal degree of freedom ($D=1$), only a two-dimensional gauge degree of freedom ($N=2$) corresponding to polarization. The Hamiltonian operator $\hat{H}:\mathcal{D}_H\to\mathcal{H}$ is a quadratic polynomial of the momentum operators:

$$\hat{H}=\frac{1}{2M}\left(\hat{p}_x^2+\hat{p}_y^2\right)\otimes\hat{I}_2, \tag{19}$$

where M is the mass of the particles, and $\hat{I}_2$ is the 2×2 identity matrix.

For wave number $\mathbf{k}=k(\cos\vartheta,\sin\vartheta)$, the energy eigenvalues of the Hamiltonian in Eq. (19) are doubly degenerate and

are given by

$$E(k,\vartheta) = \frac{\hbar^2 k^2}{2M}. \tag{20}$$

One can see that the band structure is isotropic, namely, depends only on the magnitude of wave number $k = |\mathbf{k}|$, and thus, the constant energy curves are circles.

Due to the regularity requirement [28], the momentum space eigenvectors need to be chosen such that one of its components is independent of ϑ. In this case, there is only one possible choice up to a constant multiplier:

$$\mathbf{u}(k,\vartheta) = 1. \tag{21}$$

From Eqs. (13) and (20), one finds that the group velocity is

$$v_k(k,\vartheta) = \frac{\hbar k}{M}, \quad v_\vartheta(k,\vartheta) = 0. \tag{22}$$

The radial component of the group velocity is positive for all $k > 0$, implying that the single band of this model is an electronlike band. Here, we stress that the sign of the radial group velocity is relevant because it modifies the contours on the complex plane as detailed after Eq. (13).

The $\mathfrak{su}(2)$ Lie algebra corresponding to the SU(2) group is three dimensional, whose standard basis consists of the half-Pauli matrices:

$$\hat{\tau}_1 = \frac{1}{2}\begin{pmatrix} 0 & 1 \\ 1 & 0 \end{pmatrix}, \quad \hat{\tau}_2 = \frac{1}{2}\begin{pmatrix} 0 & -i \\ i & 0 \end{pmatrix},$$
$$\hat{\tau}_3 = \frac{1}{2}\begin{pmatrix} 1 & 0 \\ 0 & -1 \end{pmatrix}. \tag{23}$$

The gauge potential of this problem is given according to Eq. (2), where the SU(2)-flux $\hat{\Phi}$ or equivalently the dimensionless flux $\hat{\alpha}$ can be parameterized with a real parameter α as follows:

$$\hat{\alpha} = 2\alpha\hat{\tau}_3 = \begin{pmatrix} \alpha & 0 \\ 0 & -\alpha \end{pmatrix}. \tag{24}$$

Note that, owing to the self-adjointness of $\mathfrak{su}(2)$-generators, an arbitrary flux can be diagonalized as in Eq. (24), and a similar statement holds also for the group elements, as pointed out by Horváthy [10]. The eigenvectors of $\hat{\alpha}$ take the form:

$$\mathbf{w}_1 = \begin{pmatrix} 1 \\ 0 \end{pmatrix}, \quad \mathbf{w}_2 = \begin{pmatrix} 0 \\ 1 \end{pmatrix}, \tag{25}$$

with eigenvalues α and $-\alpha$, respectively.

We now introduce the probability density of the position corresponding to an arbitrary state $(\Psi_1, \Psi_2) \in \mathcal{H}$:

$$\varrho = \Psi_1^* \Psi_1 + \Psi_2^* \Psi_2, \tag{26}$$

and calculate the probability current density using the general formula given in our previous work [28]. Then we find

$$j_x = \frac{1}{M}\sum_{n=1}^{2}\sum_{l=1}^{2} \mathrm{Re}[\Psi_n^*(\hat{\Pi}_{x,nl}\Psi_l)], \tag{27a}$$

$$j_y = \frac{1}{M}\sum_{n=1}^{2}\sum_{l=1}^{2} \mathrm{Re}[\Psi_n^*(\hat{\Pi}_{y,nl}\Psi_l)], \tag{27b}$$

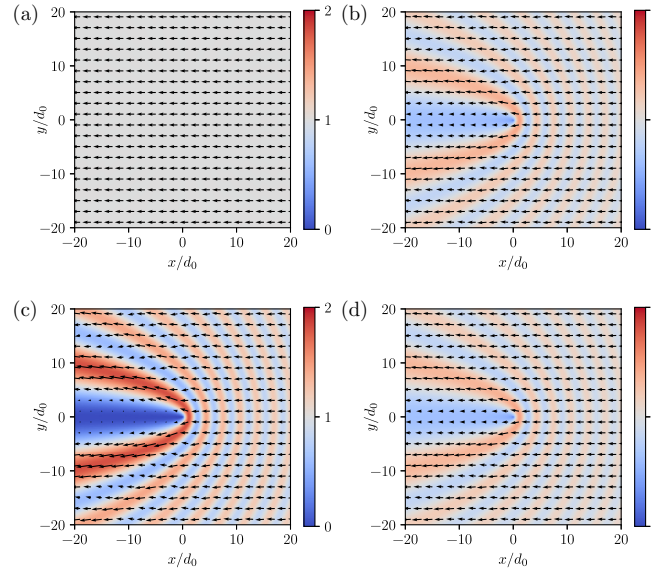

FIG. 1. Scattering states corresponding to the Aharonov-Bohm effect for the SU(2) doublet. The probability density ϱ (colors) and current density $\mathbf{j}$ (arrows) are computed for $kd_0 = 1$ (where d_0 is a natural length unit) and (a) $\alpha = 0$, (b) $\alpha = 0.2$, (c) $\alpha = 0.5$, and (d) $\alpha = 0.8$.

where $\hat{\Pi}_{x,nl}$ and $\hat{\Pi}_{y,nl}$ are the matrix elements of the kinetic momentum operators.

We now apply Eq. (11) to calculate the scattering states. The integral that appears in this expression can be simplified using the Schäfli-Sommerfeld integral formula of the Bessel functions of the first kind [33], and the final result becomes

$$\Psi^{(+)}_{1,\mathbf{k}}(r,\varphi) = \sum_{m=-\infty}^{\infty} (-i)^{|m+\alpha|} J_{|m+\alpha|}(kr) \times \exp\left[im(\varphi - \vartheta + \pi)\right]\begin{pmatrix} 1 \\ 0 \end{pmatrix}, \tag{28a}$$

for $n = 1$, and

$$\Psi^{(+)}_{2,\mathbf{k}}(r,\varphi) = \sum_{m=-\infty}^{\infty} (-i)^{|m-\alpha|} J_{|m-\alpha|}(kr) \times \exp[im(\varphi - \vartheta + \pi)]\begin{pmatrix} 0 \\ 1 \end{pmatrix}, \tag{28b}$$

for $n = 2$. Note that, for $\vartheta = 0$, these wave functions agree with the solutions obtained by Horváthy [10]; thus, this calculation serves as a checkpoint for our general method presented in this paper.

We now consider a special scattering state built as a linear combination of the wave functions in Eq. (28):

$$\Psi^{(+)} = \frac{1}{\sqrt{2}}[\Psi^{(+)}_{1,\mathbf{k}} + \Psi^{(+)}_{2,\mathbf{k}}]. \tag{29}$$

To visualize this wave function, we calculate the probability density and the current density using Eqs. (26), (27a), and (27b). The results of our numerical calculations are shown in Fig. 1.

As expected, they mostly resemble the plots obtained in the Abelian case (see, e.g., Ref. [28]) with some differences

we point out now. The most significant feature is that the scattering states are reflection symmetric with respect to the x axis. This is the consequence of the special choice of linear combination coefficients in Eq. (29). If this was not the case, then such incidental symmetry would not be present. This is clearly seen, e.g., from the scattering states of either Eq. (28a) or (28b). These possess the same probability density and current density as their Abelian counterparts and are thereby asymmetric.

Finally, we calculate the cross section factor Σ defined in Eq. (18) for the SU(2) doublet and obtain

$$\Sigma = \sin^2(\alpha\pi), \tag{30}$$

which is independent of the linear combination coefficients c_n used in Eq. (14). This shows that the differential cross section is completely insensitive to the initial state, much like in the Abelian case. However, it must be noted that this is only due to the simple nature of the SU(2) group. In the following sections, we consider more complicated cases.

B. SU(3) triplet

Our second example is the SU(3) triplet. This model is used to describe the nonrelativistic dynamics of free quarks [34,35] which participate in strong interactions via a three-state degree of freedom coupling to the gluon field, called *color* [30–32]. Although free quarks are rarely found in nature, an analogous system can be engineered using, again, ultracold atoms trapped in an optical lattice and laser-induced transitions, but here, the energy eigenstates are triply degenerate [16,17]. The non-Abelian AB effect in this system was proposed by Horváthy [10], but the calculation of the scattering states was not performed. In the following, we aim to do so using our method developed in Sec. II.

The Hilbert space corresponding to the SU(3) triplet is $\mathcal{H} = L^2(\mathbb{R}^2, \mathbb{C}) \otimes \mathbb{C}^3$, that is, there is no internal degree of freedom ($D = 1$), only a three-dimensional gauge degree of freedom ($N = 3$) corresponding to polarization. The Hamiltonian operator $\hat{H} : \mathcal{D}_H \to \mathcal{H}$ is given as a quadratic polynomial of the momentum operators:

$$\hat{H} = \frac{1}{2M}\left(\hat{p}_x^2 + \hat{p}_y^2\right) \otimes \hat{I}_3, \tag{31}$$

where M is the mass of the particles, and $\hat{I}_3$ is the 3×3 identity matrix. The above expression is formally identical to Eq. (19), although the two Hamiltonians act on different Hilbert spaces. Nevertheless, most properties of the SU(3) triplet Hamiltonian resemble those of the SU(2) doublet Hamiltonian.

The band structure corresponding to the Hamiltonian in Eq. (31) consists of a triply degenerate band which in polar coordinates (k, ϑ) of the wave number $\mathbf{k}$ is given by

$$E(k, \vartheta) = \frac{\hbar^2 k^2}{2M}. \tag{32}$$

The system is again isotropic in $\mathbf{k}$ space.

The momentum space eigenvectors are identical to that of Eq. (21):

$$\mathbf{u}(k, \vartheta) = 1. \tag{33}$$

Similarly, the group velocity field takes the same form as in Eq. (22):

$$v_k(k, \vartheta) = \frac{\hbar k}{M}, \quad v_\vartheta(k, \vartheta) = 0. \tag{34}$$

The radial component of the group velocity is positive for all $k > 0$, i.e., it is an electronlike band that is relevant to calculate the AB scattering states in Eq. (11).

The $\mathfrak{su}(3)$ Lie algebra corresponding to the SU(3) group is eight dimensional, whose standard basis consists of the Gell-Mann matrices:

$$\hat{\lambda}_1 = \begin{pmatrix} 0 & 1 & 0 \\ 1 & 0 & 0 \\ 0 & 0 & 0 \end{pmatrix}, \quad \hat{\lambda}_2 = \begin{pmatrix} 0 & -i & 0 \\ i & 0 & 0 \\ 0 & 0 & 0 \end{pmatrix},$$
$$\hat{\lambda}_3 = \begin{pmatrix} 1 & 0 & 0 \\ 0 & -1 & 0 \\ 0 & 0 & 0 \end{pmatrix}, \quad \hat{\lambda}_4 = \begin{pmatrix} 0 & 0 & 1 \\ 0 & 0 & 0 \\ 1 & 0 & 0 \end{pmatrix},$$
$$\hat{\lambda}_5 = \begin{pmatrix} 0 & 0 & -i \\ 0 & 0 & 0 \\ i & 0 & 0 \end{pmatrix}, \quad \hat{\lambda}_6 = \begin{pmatrix} 0 & 0 & 0 \\ 0 & 0 & 1 \\ 0 & 1 & 0 \end{pmatrix},$$
$$\hat{\lambda}_7 = \begin{pmatrix} 0 & 0 & 0 \\ 0 & 0 & -i \\ 0 & i & 0 \end{pmatrix}, \quad \hat{\lambda}_8 = \frac{1}{\sqrt{3}}\begin{pmatrix} 1 & 0 & 0 \\ 0 & 1 & 0 \\ 0 & 0 & -2 \end{pmatrix}. \tag{35}$$

The gauge potential of this problem is given according to Eq. (2), where the SU(3)-flux $\hat{\Phi}$ or equivalently the dimensionless flux $\hat{\alpha}$ can be parameterized with real parameters α and β as follows:

$$\hat{\alpha} = \alpha\hat{\lambda}_3 + \sqrt{3}\beta\hat{\lambda}_8 = \begin{pmatrix} \beta + \alpha & 0 & 0 \\ 0 & \beta - \alpha & 0 \\ 0 & 0 & -2\beta \end{pmatrix}. \tag{36}$$

A more generic flux could be transformed into the diagonal form of Eq. (36) by a change of basis in the $\mathbb{C}^3$ space, i.e., with a global gauge transformation. The eigenvectors of $\hat{\alpha}$ take the form:

$$\mathbf{w}_1 = \begin{pmatrix} 1 \\ 0 \\ 0 \end{pmatrix}, \quad \mathbf{w}_2 = \begin{pmatrix} 0 \\ 1 \\ 0 \end{pmatrix}, \quad \mathbf{w}_3 = \begin{pmatrix} 0 \\ 0 \\ 1 \end{pmatrix}, \tag{37}$$

with eigenvalues $\beta + \alpha$, $\beta - \alpha$, and -2β, respectively.

The probability density of the particle position corresponding to an arbitrary state $(\Psi_1, \Psi_2, \Psi_3) \in \mathcal{H}$ can be written as

$$\varrho = \Psi_1^*\Psi_1 + \Psi_2^*\Psi_2 + \Psi_3^*\Psi_3. \tag{38}$$

Applying the results of the general probability current formula of our previous paper [28], we find

$$j_x = \frac{1}{M}\sum_{n=1}^{3}\sum_{l=1}^{3}\mathrm{Re}[\Psi_n^*(\hat{\Pi}_{x,nl}\Psi_l)], \tag{39a}$$

$$j_y = \frac{1}{M}\sum_{n=1}^{3}\sum_{l=1}^{3}\mathrm{Re}[\Psi_n^*(\hat{\Pi}_{y,nl}\Psi_l)]. \tag{39b}$$

We are now ready to perform the contour integral in Eq. (11). Using the Schäfli-Sommerfeld integral formula of the Bessel functions of the first kind [33], we obtain

$$\Psi^{(+)}_{1,\mathbf{k}}(r,\varphi) = \sum_{m=-\infty}^{\infty} (-i)^{|m+\beta+\alpha|} J_{|m+\beta+\alpha|}(kr) \times \exp\left[im(\varphi-\vartheta+\pi)\right] \begin{pmatrix} 1 \\ 0 \\ 0 \end{pmatrix}, \tag{40a}$$

for $n = 1$, and

$$\Psi^{(+)}_{2,\mathbf{k}}(r,\varphi) = \sum_{m=-\infty}^{\infty} (-i)^{|m+\beta-\alpha|} J_{|m+\beta-,\alpha|}(kr) \times \exp[im(\varphi-\vartheta+\pi)] \begin{pmatrix} 0 \\ 1 \\ 0 \end{pmatrix}, \tag{40b}$$

for $n = 2$, and

$$\Psi^{(+)}_{3,\mathbf{k}}(r,\varphi) = \sum_{m=-\infty}^{\infty} (-i)^{|m-2\beta|} J_{|m-2\beta|}(kr) \times \exp\left[im(\varphi-\vartheta+\pi)\right] \begin{pmatrix} 0 \\ 0 \\ 1 \end{pmatrix}, \tag{40c}$$

for $n = 3$.

We now consider a scattering state built as a linear combination of the wave functions in Eq. (40):

$$\Psi^{(+)} = \frac{1}{\sqrt{3}}[\Psi^{(+)}_{1,\mathbf{k}} + \Psi^{(+)}_{2,\mathbf{k}} + \Psi^{(+)}_{3,\mathbf{k}}]. \tag{41}$$

To see the features of this scattering state, we calculate the corresponding probability density and current density using Eqs. (38), (39a), and (39b). The results of our numerical calculations are shown in Fig. 2.

As expected, they mostly resemble the plots acquired in the Abelian case and for the SU(2) doublet; let us now point out the differences. Depending on the values of α and β, the reflection symmetry with respect to the x axis is either present or not. Examples of the former can be seen in Figs. 2(c) or 2(f), whereas examples of the latter are in Figs. 2(b) or 2(g).

Another interesting feature is seen in Fig. 2(h), namely, for $\alpha = \beta = 0.5$, no scattering is observed, like in the case of integer α in the Abelian AB effect. This is, of course, not at all surprising since, with these parameters, all three eigenvalues of the SU(3)-flux $\hat{\alpha}$ in Eq. (36) are integers, leading to the absence of scattering in all components.

Finally, we calculate the cross section factor Σ defined in Eq. (18) for a general incoming plane wave according to Eq. (14) using the states in Eqs. (40), and we obtain

$$\Sigma = |c_1|^2 \sin^2[(\beta+\alpha)\pi] + |c_2|^2 \sin^2[(\beta-\alpha)\pi] + |c_3|^2 \sin^2[2\beta\pi], \tag{42}$$

which now depends on the linear combination coefficients c_n. A few examples of Σ for incident waves with different c_n values are shown in Fig. 3.

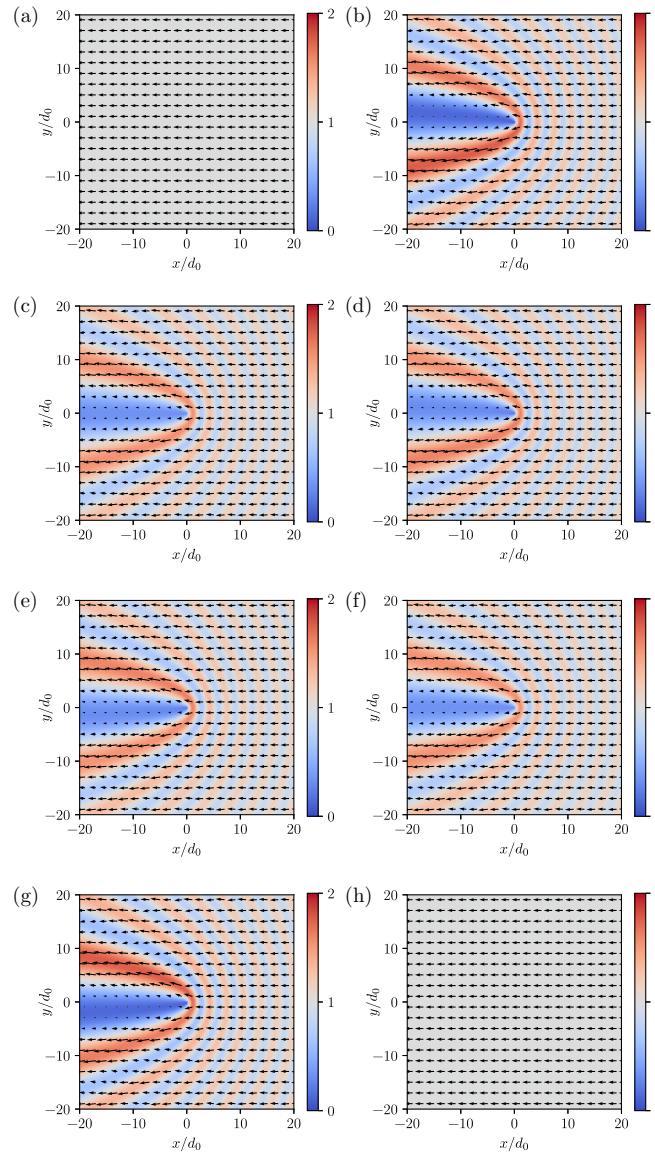

FIG. 2. Scattering states corresponding to the Aharonov-Bohm effect for the SU(3) triplet. The probability density ϱ (represented by the colors) and current density $\mathbf{j}$ (represented by the arrows) are computed for $kd_0 = 1$ (where d_0 is a natural length unit) and (a) $\alpha = \beta = 0$, (b) $\alpha = 0$, $\beta = \frac{1}{3}$, (c) $\alpha = 0$, $\beta = 0.5$, (d) $\alpha = 0.2$, $\beta = \frac{1}{3}$, (e) $\alpha = 0.3$, $\beta = \frac{1}{6}$, (f) $\alpha = 0.5$, $\beta = 0$, (g) $\alpha = 0.5$, $\beta = \frac{1}{6}$, and (h) $\alpha = 0.5$, $\beta = 0.5$.

We now discuss the details of these results. The most symmetric case is shown in Fig. 3(a), where the three polarizations are present with equal weight. One can see that the hexagonal structure in the magnitude of Σ is distorted as the coefficients c_n are changed, as shown in Figs. 3(b)–3(d). Irrespective of weights c_n, the differential cross section shows periodicity with period 1 in both α and β, and it vanishes at $\alpha, \beta \in \mathbb{R}$, like in the Abelian case. However, there is also a nontrivial zero value of the cross section factor Σ at $\alpha = \beta = 0.5$, in agreement with Fig. 2(h). Finally, we should mention that the maximal value of Σ generally does not reach unity, which is best seen in Fig. 3(a) but can be observed in other cases as well.

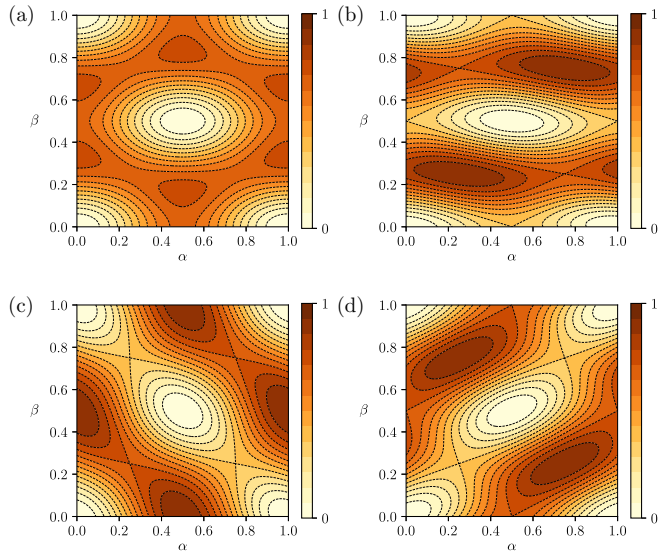

FIG. 3. Dimensionless cross section factor for the SU(3) triplet as a function of α and β for (a) $c_1 : c_2 : c_3 = 1 : 1 : 1$, (b) $c_1 : c_2 : c_3 = 1 : 2 : 3$, (c) $c_1 : c_2 : c_3 = 2 : 3 : 1$, and (d) $c_1 : c_2 : c_3 = 3 : 1 : 2$. The relation $|c_1|^2 + |c_2|^2 + |c_3|^2 = 1$ is always satisfied.

C. U(2) doublet

The third example we consider here is the U(2) doublet. From our point of view, this is equivalent to its locally isomorphic counterpart, the SU(2)×U(1) doublet, appearing in a model of K^+ and K^0 kaons where they are regarded as different isospin-hypercharge eigenstates of the same particle [30–32]. For the sake of simplicity and brevity, we use the ultrarelativistic limit, i.e., the masses of kaons are neglected in our model. However, we should note that the generic relativistic regime can also be treated in our theory. An analogous system can be engineered using, again, ultracold atoms [21,22] trapped in an optical honeycomb lattice mimicking monolayer graphene [14]. In the low-energy regime of this system, the dispersion relation resembles that of a massless relativistic particle. In what follows, we apply our methods developed in Sec. II to study the nature of the scattering wave functions and the differential cross section.

The Hilbert space corresponding to the U(2) doublet is $\mathcal{H} = L^2(\mathbb{R}^2, \mathbb{C}) \otimes \mathbb{C}^4$, that is, there is a two-dimensional internal degree of freedom ($D = 2$) and a two-dimensional gauge degree of freedom ($N = 2$) corresponding to polarization. The Hamiltonian operator $\hat{H} : \mathcal{D}_H \to \mathcal{H}$ is given as a linear polynomial of the momentum operators:

$$\hat{H} = v(\hat{p}_x \otimes \hat{I}_2 \otimes \hat{\sigma}_x + \hat{p}_y \otimes \hat{I}_2 \otimes \hat{\sigma}_y), \tag{43}$$

where v is an effective velocity parameter, and

$$\hat{\sigma}_x = \begin{pmatrix} 0 & 1 \\ 1 & 0 \end{pmatrix}, \quad \hat{\sigma}_y = \begin{pmatrix} 0 & -\mathrm{i} \\ \mathrm{i} & 0 \end{pmatrix}, \quad \hat{\sigma}_z = \begin{pmatrix} 1 & 0 \\ 0 & -1 \end{pmatrix} \tag{44}$$

are the Pauli matrices.

The band structure corresponding to the Hamiltonian in Eq. (43) consists of two doubly degenerate bands with band index $s \in \{-1, 1\}$ which in $\mathbf{k}$-space polar coordinates are given by

$$E_s(k, \vartheta) = sv\hbar k. \tag{45}$$

As before, the dispersion relation is isotropic.

The momentum space eigenvectors need to be chosen such that one of their components is independent of ϑ. This is related to the regularity of the wave function at the origin, as discussed in detail in our previous work [28]. Thus, for simplicity, we choose the following eigenvector:

$$\mathbf{u}_s(k, \vartheta) = \frac{1}{\sqrt{2}} \begin{pmatrix} 1 \\ se^{i\vartheta} \end{pmatrix}. \tag{46}$$

Then from Eqs. (13) and (45), the group velocity is given by

$$v_{s,k}(k, \vartheta) = sv, \quad v_{s,\vartheta}(k, \vartheta) = 0. \tag{47}$$

Now, it is clear that the radial group velocity for all k is either positive or negative depending on the band index s. This implies that the band with $s = 1$ is electronlike, whereas the band with $s = -1$ is holelike.

The u(2) Lie algebra corresponding to the U(2) group is four dimensional, whose standard basis consists of the half-Pauli and half-identity matrices:

$$\hat{\tau}_1 = \frac{1}{2}\begin{pmatrix} 0 & 1 \\ 1 & 0 \end{pmatrix}, \quad \hat{\tau}_2 = \frac{1}{2}\begin{pmatrix} 0 & -i \\ i & 0 \end{pmatrix},$$
$$\hat{\tau}_3 = \frac{1}{2}\begin{pmatrix} 1 & 0 \\ 0 & -1 \end{pmatrix}, \quad \hat{\tau}_4 = \frac{1}{2}\begin{pmatrix} 1 & 0 \\ 0 & 1 \end{pmatrix}. \tag{48}$$

The gauge potential of this problem is given according to Eq. (2), where the U(2)-flux $\hat{\Phi}$ or equivalently the dimensionless flux $\hat{\alpha}$ can be parameterized with real parameters α and β as follows:

$$\hat{\alpha} = 2\alpha\hat{\tau}_3 + 2\beta\hat{\tau}_4 = \begin{pmatrix} \beta + \alpha & 0 \\ 0 & \beta - \alpha \end{pmatrix}, \tag{49}$$

and the eigenvectors of $\hat{\alpha}$ are

$$\mathbf{w}_1 = \begin{pmatrix} 1 \\ 0 \end{pmatrix}, \quad \mathbf{w}_2 = \begin{pmatrix} 0 \\ 1 \end{pmatrix}, \tag{50}$$

with eigenvalues $\beta + \alpha$ and $\beta - \alpha$, respectively. A more generic flux could be transformed into the diagonal form of Eq. (49) by a change of basis in the $\mathbb{C}^2$ space, i.e., a global gauge transformation.

Then the probability density of the particle position corresponding to an arbitrary state $\mathbf{\Psi} = (\Psi_1, \Psi_2, \Psi_3, \Psi_4) \in \mathcal{H}$ can be written as

$$\varrho = \Psi_1^*\Psi_1 + \Psi_2^*\Psi_2 + \Psi_3^*\Psi_3 + \Psi_4^*\Psi_4. \tag{51}$$

Now, using the results of the general probability current formula in our previous paper [28], we find

$$j_x = 2v\ \mathrm{Re}(\Psi_1^*\Psi_2 + \Psi_3^*\Psi_4), \tag{52a}$$
$$j_y = 2v\ \mathrm{Im}(\Psi_1^*\Psi_2 + \Psi_3^*\Psi_4). \tag{52b}$$

Performing the contour integral in Eq. (11) using, again, the Schäfli-Sommerfeld integral formula of the Bessel functions of the first kind [33], we obtain the following scattering wave

functions:

$$\Psi^{(+)}_{1,1,\mathbf{k}}(r,\varphi)=\sum_{m=-\infty}^{\infty}\frac{(-i)^{|m+\beta+\alpha|}\exp[im(\varphi-\vartheta+\pi)]}{\sqrt{2}}\begin{pmatrix}J_{|m+\beta+\alpha|}(kr)\\ i\epsilon(m+\beta+\alpha)J_{|m+\beta+\alpha|+\epsilon(m+\beta+\alpha)}(kr)e^{i\varphi}\\ 0\\ 0\end{pmatrix}, \tag{53a}$$

for $s=1, n=1$,

$$\Psi^{(+)}_{-1,1,\mathbf{k}}(r,\varphi)=\sum_{m=-\infty}^{\infty}\frac{i^{|m+\beta+\alpha|}\exp[im(\varphi-\vartheta+\pi)]}{\sqrt{2}}\begin{pmatrix}J_{|m+\beta+\alpha|}(kr)\\ -i\epsilon(m+\beta+\alpha)J_{|m+\beta+\alpha|+\epsilon(m+\beta+\alpha)}(kr)e^{i\varphi}\\ 0\\ 0\end{pmatrix}, \tag{53b}$$

for $s=-1, n=1$,

$$\Psi^{(+)}_{1,2,\mathbf{k}}(r,\varphi)=\sum_{m=-\infty}^{\infty}\frac{(-i)^{|m+\beta-\alpha|}\exp[im(\varphi-\vartheta+\pi)]}{\sqrt{2}}\begin{pmatrix}0\\ 0\\ J_{|m+\beta-\alpha|}(kr)\\ i\epsilon(m+\beta-\alpha)J_{|m+\beta-\alpha|+\epsilon(m+\beta-\alpha)}(kr)e^{i\varphi}\end{pmatrix}, \tag{53c}$$

for $s=1, n=2$, and

$$\Psi^{(+)}_{-1,2,\mathbf{k}}(r,\varphi)=\sum_{m=-\infty}^{\infty}\frac{i^{|m+\beta-\alpha|}\exp[im(\varphi-\vartheta+\pi)]}{\sqrt{2}}\begin{pmatrix}0\\ 0\\ J_{|m+\beta-\alpha|}(kr)\\ -i\epsilon(m+\beta-\alpha)J_{|m+\beta-\alpha|+\epsilon(m+\beta-\alpha)}(kr)e^{i\varphi}\end{pmatrix}, \tag{53d}$$

for $s=-1, n=2$. This result is another nontrivial application of our general method.

Now, we consider a special wave function built as a linear combination of Eqs. (53a) and (53c):

$$\Psi^{(+)}=\frac{1}{\sqrt{2}}[\Psi^{(+)}_{1,1,\mathbf{k}}+\Psi^{(+)}_{1,2,\mathbf{k}}]. \tag{54}$$

Now, again using Eqs. (51) and (52), we calculate the probability density and current density, respectively, and the results are shown in Fig. 4. As we expected, these are like the wave functions of the Abelian case and the SU(2) doublet. However, a few differences should be pointed out. First, in Fig. 4(h), for parameters $\alpha=\beta=0.5$, no scattering is observed, as with the SU(3) triplet discussed in Sec. III B. This is clear because, for these parameters, the eigenvalues of the dimensionless U(2)-flux $\hat{\alpha}$ in Eq. (49) are integers resulting in the absence of scattering in all components.

Finally, we calculate the cross section factor Σ defined in Eq. (17) for the U(2) doublet and obtain

$$\Sigma=|c_1|^2\sin^2[(\beta+\alpha)\pi]+|c_2|^2\sin^2[(\beta-\alpha)\pi], \tag{55}$$

which is again dependent on the linear combination coefficients c_n. A few examples regarding different incident waves are shown in Fig. 5.

The following general features of Σ can be observed as the coefficients c_n of the incoming waves are changed. The tetragonal structure in the magnitude of Σ shown in Fig. 5(a) will be distorted as the ratio of c_1/c_2 is changed, as clearly seen in Figs. 5(b) and 5(c). Again, irrespective of c_1 and c_2, the differential cross section shows a periodicity with period 1 in both α and β, and it vanishes at $\alpha,\beta\in\mathbb{R}$ and $\alpha=\beta=0.5$, as with the SU(3) triplet. Moreover, the maximal value of the cross section factor Σ is always unity if $\alpha+\beta$ and $\alpha-\beta$ are half-integers. Actually, this feature is rather different from the case of the SU(3) triplet. Finally, an interesting feature can be observed by comparing Figs. 5(b) and 5(c): Those are reflections of each other as a result of the symmetric partition of weights, that is, $c_1/c_2=2$ or $c_2/c_1=2$.

IV. CONCLUSIONS

To conclude, for the non-Abelian AB effect in isotropic multiband systems, we have two central results: first, the contour integral representation of the scattering states and, second, the differential scattering cross section, given in Eqs. (11) and (17), respectively. The form of the scattering states is a natural extension of that established for the Abelian AB problem in our recent work [28].

Like in the Abelian case, our proposed wave functions satisfy the necessary boundary and regularity. Moreover, using the asymptotic form of the non-Abelian scattering states given by Eq. (11), we obtained the differential scattering cross section which has the following main features. First, the angular dependence of the cross section is the same as that obtained by Aharonov and Bohm [1]. Second, in contrast to the Abelian case, we found that the cross section now depends

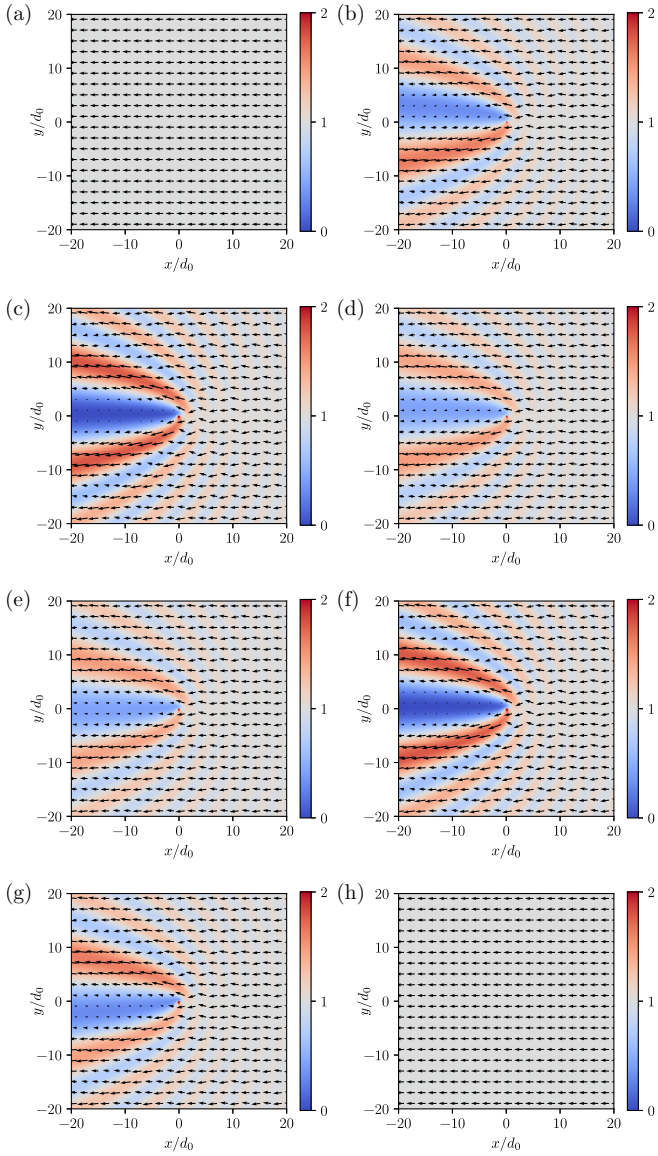

FIG. 4. Scattering states corresponding to the Aharonov-Bohm effect for the U(2) doublet. The probability density ϱ (represented by the colors) and current density $\mathbf{j}$ (represented by the arrows) are computed for $kd_0 = 1$ (where d_0 is a natural length unit) and (a) $\alpha = \beta = 0$, (b) $\alpha = 0$, $\beta = 0.25$, (c) $\alpha = 0$, $\beta = 0.5$, (d) $\alpha = 0.2$, $\beta = 0.3$, (e) $\alpha = 0.3$, $\beta = 0.2$, (f) $\alpha = 0.5$, $\beta = 0$, (g) $\alpha = 0.5$, $\beta = 0.25$, and (h) $\alpha = 0.5$, $\beta = 0.5$.

on the polarization of the incoming plane wave considering the so-called cross section factor Σ given by Eq. (18).

To show how versatile our theory is, in Sec. III, we carried out the complex contour integrals in Eq. (11) for three nontrivial isotropic multiband systems relevant to condensed matter and particle physics. For each case, we obtained the explicit form of the scattering states, and to have a deeper

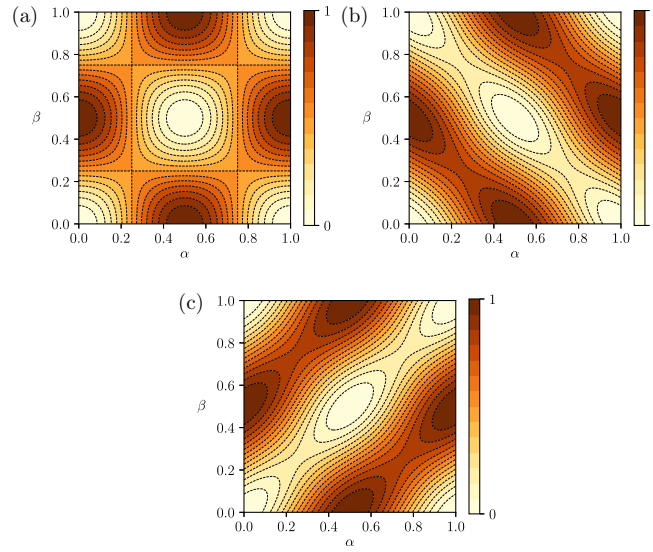

FIG. 5. Dimensionless cross section factor for the U(2) doublet as a function of α and β for (a) $c_1 : c_2 = 1 : 1$, (b) $c_1 : c_2 = 1 : 2$, and (c) $c_1 : c_2 = 2 : 1$. The relation $|c_1|^2 + |c_2|^2 = 1$ is always satisfied.

insight into their nature, we plotted their probability and current distributions for different incoming waves. We pointed out the similarities and differences between these wave functions and those of the Abelian case.

Our first example, the SU(2) doublet, serves as a test problem since it has already been studied by Wu and Yang [9] and Horváthy [10]. Indeed, our general approach gives the same scattering states as those derived by Horváthy [10]. Then in Secs. III B and III C, we calculated the wave functions for two further systems: the SU(3) triplet and the U(2) doublet, respectively. Furthermore, we calculated the cross section factor Σ for different incoming polarizations in these systems. The results show a periodic structure as a function of the flux parameters. Our general theory can easily be applied to other non-Abelian isotropic multiband systems. We believe that our work broadens the scope of the exactly solvable AB scattering problems.

ACKNOWLEDGMENTS

We thank M. Berry, P. A. Horváthy, C. Lambert, B. Dóra, and Gy. Dávid for valuable discussions. This paper was supported by the Ministry of Culture and Innovation and the National Research, Development and Innovation Office within the Quantum Information National Laboratory of Hungary (Grant No. 2022-2.1.1-NL-2022-00004), by the ÚNKP-22-3 New National Excellence Program of the Ministry for Culture and Innovation from the Source of the National Research, Development and Innovation Fund, and by the Hungarian Scientific Research Fund (OTKA) Grant No. K134437.

[1] Y. Aharonov and D. Bohm, Significance of electromagnetic potentials in the quantum theory, Phys. Rev. **115**, 485 (1959).

[2] R. G. Chambers, Shift of an electron interference pattern by enclosed magnetic flux, Phys. Rev. Lett. **5**, 3 (1960).

[3] M. V. Berry, Exact Aharonov-Bohm wavefunction obtained by applying Dirac's magnetic phase factor, Eur. J. Phys. **1**, 240 (1980).
[4] M. V. Berry, R. G. Chambers, M. D. Large, C. Upstill, and J. C. Walmsley, Wavefront dislocations in the Aharonov-Bohm effect and its water wave analogue, Eur. J. Phys. **1**, 154 (1980).
[5] M. G. Alford and F. Wilczek, Aharonov-Bohm interaction of cosmic strings with matter, Phys. Rev. Lett. **62**, 1071 (1989).
[6] Ph. de Sousa Gerbert, Fermions in an Aharonov-Bohm field and cosmic strings, Phys. Rev. D **40**, 1346 (1989).
[7] C. R. Hagen, Aharonov-Bohm scattering of particles with spin, Phys. Rev. Lett. **64**, 503 (1990).
[8] C. R. Hagen and S. Ramaswamy, Aharonov-Bohm scattering of massive spin-one particles, Phys. Rev. D **42**, 3524 (1990).
[9] T. T. Wu and C. N. Yang, Concept of nonintegrable phase factors and global formulation of gauge fields, Phys. Rev. D **12**, 3845 (1975).
[10] P. A. Horváthy, Non-Abelian Aharonov-Bohm effect, Phys. Rev. D **33**, 407 (1986).
[11] M. Bright and D. Singleton, Time-dependent non-Abelian Aharonov-Bohm effect, Phys. Rev. D **91**, 085010 (2015).
[12] S. A. Hosseini Mansoori and B. Mirza, Non-Abelian Aharonov-Bohm effect with the time-dependent gauge fields, Phys. Lett. B **755**, 88 (2016).
[13] N. Goldman, A. Kubasiak, P. Gaspard, and M. Lewenstein, Ultracold atomic gases in non-Abelian gauge potentials: The case of constant Wilson loop, Phys. Rev. A **79**, 023624 (2009).
[14] A. Bermudez, N. Goldman, A. Kubasiak, M. Lewenstein, and M. A. Martin-Delgado, Topological phase transitions in the non-Abelian honeycomb lattice, New J. Phys. **12**, 033041 (2010).
[15] A. Gorshkov, M. Hermele, V. Gurarie, C. Xu, P. Julienne, J. Ye, P. Zoller, E. Demler, M. Lukin, and A. Rey, Two-orbital SU(N) magnetism with ultracold alkaline-earth atoms, Nat. Phys. **6**, 289 (2010).
[16] R. Barnett, G. R. Boyd, and V. Galitski, SU(3) spin-orbit coupling in systems of ultracold atoms, Phys. Rev. Lett. **109**, 235308 (2012).
[17] D. Banerjee, M. Bögli, M. Dalmonte, E. Rico, P. Stebler, U.-J. Wiese, and P. Zoller, Atomic quantum simulation of $\mathbf{U}(N)$ and SU(N) non-Abelian lattice gauge theories, Phys. Rev. Lett. **110**, 125303 (2013).
[18] N. Goldman, F. Gerbier, and M. Lewenstein, Realizing non-Abelian gauge potentials in optical square lattices: An application to atomic Chern insulators, J. Phys. B: At., Mol. Opt. Phys. **46**, 134010 (2013).
[19] L. Tagliacozzo, A. Celi, P. Orland, and M. Lewenstein, Simulations of non-Abelian gauge theories with optical lattices, Nat. Commun. **4**, 2615 (2013).
[20] E. Zohar, J. I. Cirac, and B. Reznik, Cold-atom quantum simulator for SU(2) Yang-Mills lattice gauge theory, Phys. Rev. Lett. **110**, 125304 (2013).
[21] K. Osterloh, M. Baig, L. Santos, P. Zoller, and M. Lewenstein, Cold atoms in non-Abelian gauge potentials: From the Hofstadter "Moth" to lattice gauge theory, Phys. Rev. Lett. **95**, 010403 (2005).
[22] A. Jacob, P. Ohberg, G. Juzeliunas, and L. Santos, Cold atom dynamics in non-Abelian gauge fields, Appl. Phys. B **89**, 439 (2007).
[23] J. Dalibard, F. Gerbier, G. Juzeliunas, and P. Ohberg, Colloquium: Artificial gauge potentials for neutral atoms, Rev. Mod. Phys. **83**, 1523 (2011).
[24] N. Goldman, G. Juzeliūnas, P. Öhberg, and I. B. Spielman, Light-induced gauge fields for ultracold atoms, Rep. Prog. Phys. **77**, 126401 (2014).
[25] M.-X. Huo, W. Nie, D. A. W. Hutchinson, and L. C. Kwek, A solenoidal synthetic field and the non-Abelian Aharonov-Bohm effects in neutral atoms, Sci. Rep. **4**, 5992 (2014).
[26] M. Aidelsburger, S. Nascimbene, and N. Goldman, Artificial gauge fields in materials and engineered systems, C. R. Phys. **19**, 394 (2018).
[27] Y. Yang, C. Peng, D. Zhu, H. Buljan, J. D. Joannopoulos, B. Zhen, and M. Soljačić, Synthesis and observation of non-Abelian gauge fields in real space, Science **365**, 1021 (2019).
[28] R. Németh and J. Cserti, Unified description of the Aharonov-Bohm effect in isotropic multiband electronic systems, Phys. Rev. Res. **5**, 023154 (2023).
[29] W. Heisenberg, Über den Bau der Atomkerne. I., Z. Phys. **77**, 1 (1932).
[30] T.-P. Cheng and L.-F. Li, *Gauge Theory of Elementary Particle Physics* (Oxford University Press, Oxford, 1984).
[31] O. Nachtmann, A. Lahee, and W. Wetzel, *Elementary Particle Physics: Concepts and Phenomena* (Springer, Berlin, Heidelberg, 2012).
[32] D. Horváth and Z. Trócsányi, *Introduction to Particle Physics* (Cambridge Scholars Publishing, Cambridge, 2019).
[33] A. Erdélyi, W. Magnus, F. Oberhettinger, and F. G. Tricomi, *Higher Transcendental Functions*, Vol. II (McGraw-Hill Book Company, Inc., New York-Toronto-London, 1953).
[34] M. Gell-Mann, A schematic model of baryons and mesons, Phys. Lett. **8**, 214 (1964).
[35] G. Zweig, *An* SU_3 Model for strong interaction symmetry and its breaking; version 1, Tech. Rep. (CERN, Geneva, 1964) an updated version of the paper is available as CERN-TH-412, 1964.